ELSEVIER

Journal of Organometallic Chemistry 538 (1997) 9–17

Journal of Organometallic Chemistry

Structure and stereodynamic relationships in (η^4-diene)ML_3 systems

Patrick McArdle [a,*], Joseph Skelton [a], Anthony R. Manning [b]

[a] *Chemistry Department, University College, Galway, Ireland*
[b] *Chemistry Department, University College, Belfield, Dublin 4, Ireland*

Received 22 April 1996; revised 27 October 1996

Abstract

A structure analysis of the change in geometry from square base pyramidal to trigonal bipyramidal has been derived for over 40 (η^4-diene)ML_3 systems. This relationship is closely followed and suggests that a Berry type mechanism for intramolecular ligand exchange is possible in these systems. The nature of one element of the alternative turnstile barrier has been examined using extended Hückel calculations.

Keywords: Berry; Tricarbonyliron; Diene

1. Introduction

The well known square based pyramidal structure first established for (η^4-butadiene)$Fe(CO)_3$ has been applied, often without any structural evidence, to other (η^4-diene)ML_3 systems. The dynamic nature of these five-coordinate structures has been examined by variable temperature IR and NMR methods. These results have been interpreted in terms of axial–basal ligand site exchange within the square pyramidal structure via a turnstile mechanism [1–4]. Recent structural work has emphasised the close approach to trigonal bipyramidal geometry that is often observed in these systems [5]. This alternative structural type raises the possible involvement of Berry type stereodynamics.

2. Structure of (η^4-diene)ML_3 systems

The square base pyramidal structure (SQP) of (η^4-butadiene)$Fe(CO)_3$ [6] has been observed for many related complexes of conjugated dienes, it has also been applied to both conjugated and non-conjugated systems (as the most likely structure) in cases where no crystallographic evidence was available [1,7–9]. The alternative trigonal bipyramidal structure (TBP) has been observed in some non-conjugated cases [10]. However, it was the observation that a conjugated diene complex could adopt the TBP arrangement as its ground state structure that suggested a more detailed look at (η^4-diene)ML_3 structures was necessary [5].

The structures analysed are classified into four basic types. The first group (C*n*) contains the conjugated polyene complexes, Fig. 1. The second group (NCP*n*) contains the polyenes whose double bonds are non-conjugated and parallel to each other. Examples involve 1,5-cyclooctadiene (NCP1) and norbornadiene (NCP2 and NCP3). The third group (NCNP*n*) contains polyenes where the π-bonded olefin groups are non-conjugated and also non-parallel. The final group (M*n*) contains novel polyenes included to establish the behaviour of cases where the TBP geometry is likely to be strongly favoured. The contrast between the C*n* and NCP*n* structural types is strikingly demonstrated if the structures of (η^4-norbornadiene)$Fe(CO)_2CNMe$ [10] (a distorted trigonal bipyramid) and (η^4-butadiene)$Fe(CO)_3$ are superposed. The centroids of the double bonds and the metal atoms of both structures were fitted and the result is shown in Fig. 2 (the atoms of the butadiene structure are shown as open circles).

The overall result is that the ML_3 fragment of one structure is rotated approximately 90° from the other. The structures of conjugated diene complexes in this study all (with one exception) adopt the SQP geometry. A simple test of the resistance of this geometry to steric effects is provided by the PPh_3 substituted complexes [11] (C1 and C4), Fig. 3.

* Corresponding author.

PII S0022-328X(96)06904-5

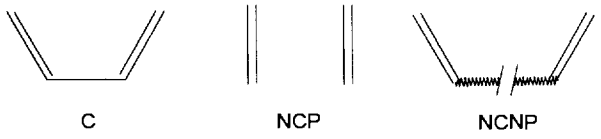

Fig. 1. Compound classification by diene type.

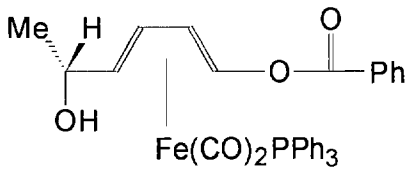

C1

The complex was isolated as a separable mixture of diastereoisomers, one of which crystallised with two molecules per asymmetric unit with the bulky PPh_3 group in both apical and basal positions. The superposition of these two structures, C1 and C4, Fig. 3, was achieved by fitting the η^4-diene carbons and the metal atoms from each structure, and the fit is good. The close approach of C1 and C4 to the butadiene structure, C10, is shown in Fig. 4, where C4 and C10 are fitted. To quantify these empirical observations a Berry plot [12] for the transition from SQP geometry to TBP geometry was constructed.

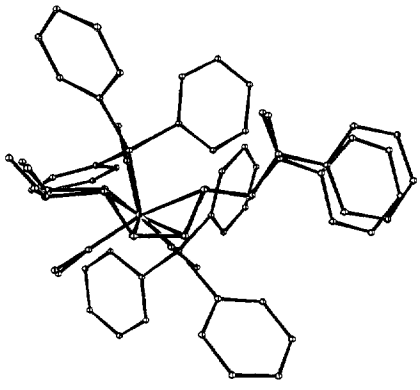

Fig. 3. Superposition of C1 (PPh_3 apical) and C4 (PPh_3 basal).

3. Berry plot

While all of the structures analysed in this study are formally five-coordinate, some of these structures are best viewed as trigonal bipyramids while others are more appropriately viewed as square based pyramids. There are three steps in the measurement procedure used to generate the data for the Berry plot. These were the identification of the 'unique' monodentate ligand, the measurement of interligand angles θ and interfacial angle δ. The first step establishes a definite relationship between the trigonal bipyramidal and square pyramidal structures by defining one of the monodentate ligands as unique, labelled * in Fig. 5. The method used to identify this unique ligand is described in Section 5. The model structure in Fig. 5 is a trigonal bipyramid or square based pyramid depending on the values of the angles 1–M–5 and 2–M–4, $\theta_{1,5}$ and $\theta_{2,4}$ respectively. In an ideal square based pyramid $\theta_{1,5}$ and $\theta_{2,4}$ are equal (150°) and in a regular trigonal bipyramid they are 180° and 120° respectively. The remaining parameter $\delta_{2,4}$ is the angle between the normals to the faces defined by the ligands 1,2,4 and 5,2,4. These faces define planes which intersect along the 2,4 line. More details are given in Section 5. A Berry plot may be constructed by plotting $\delta_{2,4}$ against $\theta_{2,4}$ or $\theta_{1,5}$.

Since typical dienes do not have bite angles of 90°, it is inevitable that TBP structures will be distorted. However, this distortion does not have an equal effect on $\theta_{2,4}$ and $\theta_{1,5}$. In all cases examined the distortion has a much greater effect on $\theta_{1,5}$ than on $\theta_{2,4}$. This is clearly due to unequal metal–olefin bonding in the axial and equatorial sites. This is expected as Hoffmann and

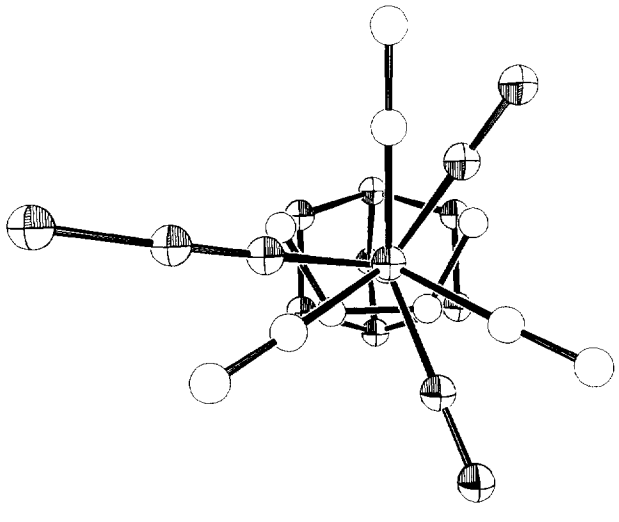

Fig. 2. Superposition of C10 and NCP4.

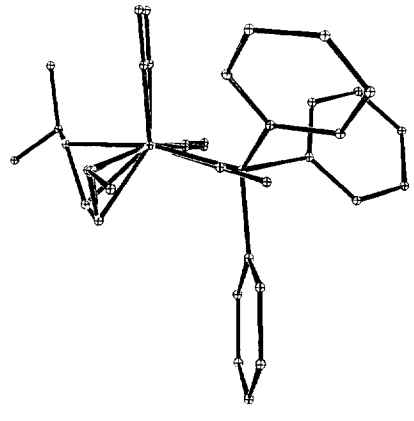

Fig. 4. Superposition of C4 and C10.

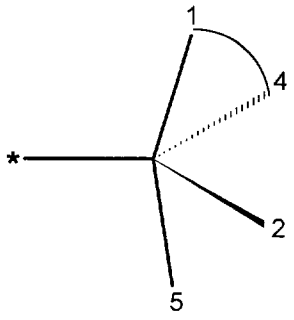

Fig. 5. Ligand identification in (diene)Fe(CO)$_3$.

coworker [13] have calculated that an olefin will bond preferentially in the equatorial position where stronger π-bonding is available. The result of this unequal bonding is that plots based on $\theta_{1,5}$ data will be less reliable. Published Berry plots for five-coordinate systems do not encounter this problem as they all involve compounds with σ-bonding ligands [14]. To extend Berry plots to η^4-diene complexes the restrictions imposed by this bonding mode had to be accommodated. All measurements were made on X-ray crystal structures, and to ensure that the analysis was performed in a totally objective way a non-subjective method was adopted for the choice of geometrical parameters.

An ideal trigonal bipyramid (five atoms surrounding a central atom) requires 12 parameters ($3N-6$) to fully describe the geometry of the molecule [15]. Clearly the representation of this type of structure using fewer than $3N-6$ geometrical parameters demands that the same parameters are measured for each structure and also necessitates assumptions relating to the independence of the remaining parameters. Berry data is given in Table 1 and references and structure identifications in Table 2. A plot of the $\theta_{2,4}$ data is given in Fig. 6. The dotted line

Table 1
Berry plot data

Label	$\delta_{2,4}$ (°)	$\theta_{2,4}$ (°)	$\theta_{1,5}$ (°)	Label	$\delta_{2,4}$ (°)	$\theta_{2,4}$ (°)	$\theta_{1,5}$ (°)
NCP1	1.1	154.0	154.0	C19	19.3	140.3	148.2
NCNP1	3.2	147.8	150.0	C20	19.4	143.1	145.0
C1	9.7	141.8	147.6	C21	19.7	144.0	159.9
NCNP2	9.9	147.9	155.4	C22	19.7	143.2	145.7
C2	14.5	146.6	148.1	C23	19.8	143.6	143.9
C3	14.9	139.1	143.8	NCNP3	19.9	142.3	162.1
C4	16.2	142.9	143.2	C24	20.2	142.9	146.0
C5	16.3	147.6	148.4	C25	20.2	139.0	146.4
C6	16.5	140.6	147.1	C26	20.7	141.0	148.5
C7	16.7	143.6	144.1	C27	20.9	143.3	145.3
C8	16.8	142.9	146.9	C28	21.0	142.3	143.5
NCP2	17.3	143.3	155.8	C29	24.8	139.6	155.0
C9	17.6	143.9	145.6	C30	24.9	137.3	154.0
C10	17.7	145.9	145.9	C31	25.8	139.7	141.3
C11	17.9	141.4	144.2	C32	27.3	138.0	138.5
C12	17.9	141.0	143.0	C33	27.6	131.6	154.4
C13	18.0	144.9	145.1	NCP3	34.7	134.7	160.1
C14	18.1	142.6	144.7	NCNP4	37.1	131.0	164.3
C15	18.4	145.2	147.2	NCP4	40.1	129.7	167.5
C16	18.8	143.6	146.5	M1	42.3	132.6	172.9
C17	19.0	143.2	148.9	M2	47.3	123.6	169.3
C18	19.3	140.2	147.3	NCP5	47.9	122.5	166.8
C19	19.3	140.3	148.2				

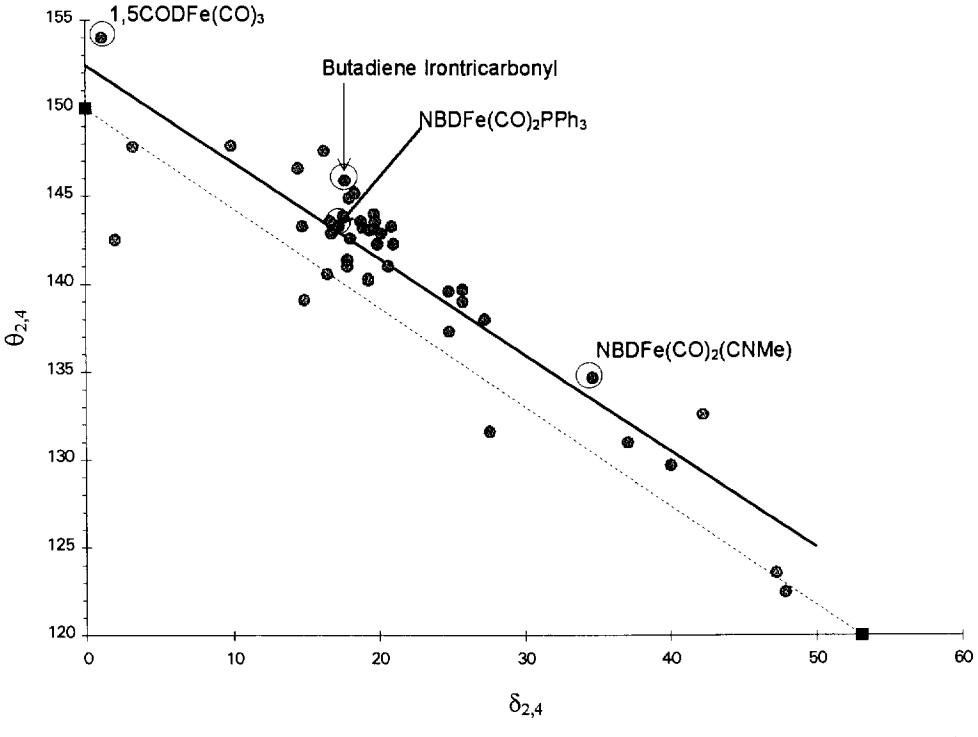

Fig. 6. Berry plot of $\theta_{2,4}$ vs. $\delta_{2,4}$, the solid line is a least-squares fit to the data and the dotted line is the theoretical Berry line. NBD = norbornadiene.

Table 2
Compound names and references

Label	Name	Ref
NCP1	Tricarbonyl(η^4-cycloocta-1,5-diene)iron	[1]
NCNP1	Tricarbonyl(η^4-tricyclo(5.3.1.0-4,9)undeca-2,5-diene)iron	[23]
C1	Dicarbonyltriphenylphosphine(η^4-hexa-1,3-diene-5-ol benzoate)iron (P apical)	[24]
NCNP2	Tricarbonyl(1,1-dimethyl-4-phenyl-1-sila-4-bora-2,5-cyclohexa-1,3-diene)iron	[25]
C2	Tricarbonyl(η^4cyclodeca-1,3,5,7-tetraene)iron	[26]
C3	Dicarbonyltriphenylphosphine(η^4-hepta-3,5-diene-2-one)iron	[24]
C4	Dicarbonyltriphenylphosphine(η^4-hexa-1,3-diene-5-ol benzoate)iron (P basal)	[24]
C5	Tricarbonyl(η^4-*exo*-2-methoxy-5,6-dimethylene-*syn*-7-norbornanol)*endo*-iron	[27]
C6	Carbonyltrimethylphosphitetriphenylphosphine(η^4-hexa-2,4-diene-1-al)iron (-143 °C)	[28]
C7	Tricarbonyl(η^4-5,6-dimethylidene-2-*exo*-norbornyl-p-bromobenzoate)iron	[29]
C8	Tricarbonyl(η^4-(N-methoxycarbonyl)azepine)iron	[30]
NCP2	Dicarbonyldiphenylphosphine(η^4-bicyclo(2.2.1)hepta-2,5-diene)iron	[10]
C9	Tricarbonyl(η^4-buta-1,3-diene-1-(phenylcarboxy)-4-(3,4-dimethyl-5-phenyloxazole)iron	[31]
C10	Tricarbonyl(η^4-buta-1,3-diene)iron	[6]
C11	Tricarbonyl(η^4-(7,7,8,8-tetracyano)bicyclo(4.2.1)nona-2,4-diene)iron	[32]
C12	Dicarbonyl(L(+)neomenthyl)diphenylphosphine(η^4-penta-1,3-diene carbomethoxy)iron	[33]
C13	Tricarbonyl(η^4-7-phenyl cyclohepta-1,3,5-triene)iron	[34]
C14	Tricarbonyl(η^4-5-(methoxy)-penta-2,3-dieneone)iron	[31]
C15	Tricarbonyl(η^4-(7-styryl)cyclohepta-1,3,5-triene)iron	[35]
C16	Tricarbonyl(η^4-azepine)iron	[36]
C17	Dicarbonyltriphenylphosphine(η^4-(N-ethoxycarbonyl)azepine)iron	[37]
C18	Dicarbonyltriphenylphosphine(η^4-cyclohexadiene)iron	[38]
C19	Dicarbonyltriphenylphosphine(η^4-hexa-3,5-diene-2-one)iron	[37]
C20	Ticarbonyl(η^4-1,2,3,4-tetramethyl-5,6-bis(trifluoromethyl)benzene)iron	[39]
C21	Carbonyltriphenylphosphinetrimethylphosphite(η^4-2-methylbuta-1,3-diene)iron	[28]
C22	Tricarbonyl(η^4-N-ethoxy-3-formylazepine)iron ([40], previous structure)	[37]
C23	Tricarbonyl(η^4-α-methylstyrene)iron	[41]
NCNP3	Dicarbonyl(4-methyl-2,6,7-trioxaphosphabicyclo(2.2.2)octane)(η^4-1,2,3,8-tetra-(trifluoromethyltricyclo(6.3.0.0-4,11)undeca-2,5-diene)iron	[42]
C24	Tricarbonyl(η^4-dimethylenecyclohexa-3,5-diene)iron (-120 °C)	[43]
C25	Dicarbonyl(L(+)neomenthyldiphenylphosphine)(η^4-(carbomethoxybuta-1,3-diene)iron	[24]
C26	Tricarbonyl(η^4-3-acetylazepine)iron	[44]
C27	Carbonyltriphenylphosphinetrimethylphosphite(η^4-buta-1,3-diene)iron	[28]
C28	Tricarbonyl(η^4-3,5-dimethoxy-α-methylcyclohexa-2,4-diene-1β-carboxylate)iron	[45]
C29	Tricarbonyl(η^4-dimethyl-4-methyl-1-oxo-penta-1,3-diene-2,3-dicarboxylate)iron	[46]
C30	Tricarbonyl(2,4-dimethylpenta-1,3-dieneone)iron	[47]
C31	Tricarbonyl(η^4-2,5-methanobicyclo(4.3.0)-nona-6,9-diene-8-spiro-cyclopentane)iron	[48]
C32	Dicarbonyltriphenylphosphine(η^4-(2,4-diphenylbicyclo(3.3.0)octa-1,4-diene-3-one)iron	[49]
C33	Bis(dicarbonyl(2,3-dimethyl-buta-1,3-diene)cobalt)(μ-dichlorotin(II))	[5]
NCP3	Tricarbonyl(η^4-dicyanobicyclo(2.2.2)octa-2,5-diene)iron	[50]
NCP4	Dicarbonylmethylisocyanide(η^4-(bicyclo(2.2.1)hepta-2,5-diene)iron	[10]
NCNP4	Tricarbonyl(η^4-2-isopropylthio-8-benzoylbicyclo(3.2.1)octadiene)iron	[51]
NCP5	Tricarbonyl(η^4-dimethylnorborna-2,5-diene-2,3-dicarboxylate)iron	[52]
M1	Tricarbonyl-bis(η^2-*trans*-cyclooctene)iron	[2]
M2	Tricarbonyl(η^4-1,5-dimethylene-2,6-dimethylcyclooctane)iron	[53]
NCP6	Tricarbonyl(η^4-dimethylbicyclo(2.2.2)octa-2,5-dienedicarboxylate)iron	[50]

represents the theoretical Berry coordinate, i.e. the θ and δ values for the ideal Berry pseudo-rotation. The solid line is the linear least-squares fit of the data. The $\theta_{2,4}$ data (in contrast to that for $\theta_{1,5}$) follows the Berry line quite well, having a linear correlation coefficient of 0.90. The least-squares line has a slight positive bias relative to the theoretical Berry line. This difference is due to the fact that the theoretical line assumes that the *trans* basal angles in a square base pyramid are 150°. In practise however the *trans* basal angles in a real square based pyramidal structure are slightly greater than 150° ((η^4-1,5-cyclooctadiene)$Fe(CO)_3$, the most square based pyramidal complex in this study, has *trans* basal angles of 154°). This is also in accord with the observations of Holmes et al. [14] on silicon and phosphorus based systems, who suggested that the real *trans* basal angles are close to 152°. This angle is also close to that calculated for the square based pyramid by Zeeman [16] and Kepert [17]. It is also interesting that complexes such as NCP1 [1] and (η^4-norbornadiene)tricarbonyliron [4] (similar to NCP4), which have very low ligand interconversion barriers and exchange rates fast enough

to average IR spectra, are not localised in any region of the line. This is in contrast to the conjugated dienes (C*n*), having barriers measurable by NMR methods, which are confined to a restricted region of about 5° on the plot. While it is impossible to prove that either turnstile or Berry pseudo-rotation is the 'correct' mechanism by macroscopic methods, this microscopic method demonstrates the viability of the Berry mechanism in these systems.

It has been shown that in the case of (η^4-diene)$M(CO)_2PR_3$ systems where the diene is unsymmetrical the ^{13}CO NMR spectrum displays two peaks at temperatures up to the decomposition point of the complex [9]. While this is clearly in accord with a turnstile type mechanism it was interesting to see if a Berry type mechanism would scramble the CO groups in such a system. The result from such an analysis is that even if the Berry mechanism is allowed access to all SQP and TBP geometries including unknown types (e.g. SQP with the diene in apical and basal positions), the CO groups will still not be scrambled. Ligand scrambling in η^4-diene ML_3 systems is thus equally well explained by both turnstile and Berry mechanisms. It was decided to attempt the calculation of the ligand exchange barrier using extended Hückel methods. However, the method used, CACAO, is more suited to a calculation of the turnstile barrier rather than the Berry pseudo-rotation, as a complex combination of translation and rotation is required to model the latter.

4. Calculation of the turnstile barrier

The turnstile mechanism is often considered to be a simple rotation of an ML_3 fragment, of C_{3V} symmetry, relative to the C_n fold axis of the chelating diene [18]. However, for the turnstile mechanism to be operative in complexes of either square based pyramidal or trigonal bipyramidal geometry, some deformation of the ML_3 fragment, often of C_S symmetry, must occur. Essentially the turnstile consists of three steps: (i) deformation of ML_3 from local C_S to C_{3V} symmetry; (ii) rotation of ML_3 relative to the chelating ligand; (iii) relaxation of ML_3 from C_{3V} to C_S symmetry. The first and third steps will be of low energy relative to step two, and it is the energy of step two which is calculated here.

In all cases diene–tricarbonyliron bonding consisted of three principal interactions. These were the well known donor and acceptor interactions [19], here referred to as Donor 1, Donor 2 and Acceptor 1. The first two involve donation of the two diene electron pairs and the latter is the backbond involving donation of electron density from metal to diene. The fragment molecular

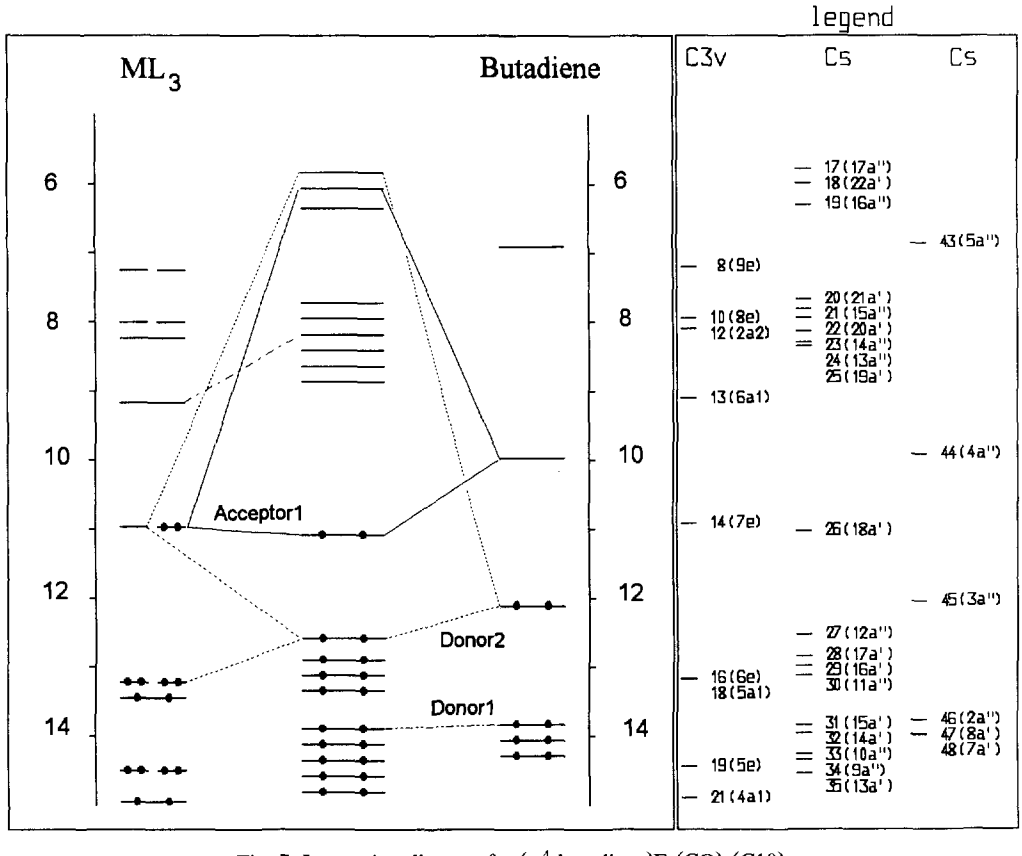

Fig. 7. Interaction diagram for (η^4-butadiene)$Fe(CO)_3$(C10).

Table 3
FMO interactions for η^4-butadiene–$Fe(CO)_3$

	$M(CO)_3$	Ligand
Acceptor 1	14 (e)	44 (a″)
Donor 2	15 (e)	45 (a″)
Donor 1	13 (a_1)	44 (a″)

orbitals (FMO) and molecular orbitals (MO) for each of the interactions are shown in Table 3. All other interactions each accounted for less than 3% of orbital overlap (based on overlap populations between frontier molecular orbitals). The results for C10 are typical and are illustrated in Fig. 7, and the overlap populations for the principal interactions in four systems are given in Table 4. Note that on the right hand side of Fig. 7 the resolution between energy levels has been enhanced for clarity, the right hand side of the figure indicates the relative energy levels of the MOs and FMOs and also gives the symmetry labels for each orbital.

The energy of the barrier was monitored by constructing Walsh diagrams, those for NCP1 and C10 are shown in Fig. 8 [20]. The dotted line in the figure shows the sum of the one electron energies throughout the rotation and the range of this value is given below each diagram in electron volts. The energy plot on the right hand side has been amplified for clarity. In the only reported calculation of a rotation barrier for these systems, Hoffmann and coworkers [7] gave a value of 7.2 kcal mol^{-1} and this compares well with the values in Table 4.

The origin of the barrier to rotation lies in the lack of an orthogonal pair of ligand orbitals in conjugated dienes. Along the series (i) cyclopentadienyl–M, (ii) NCP–M, and (iii) C–M, essentially the same pair of degenerate and orthogonal metal orbitals (iv) interacts with ligand orbitals which are (i) orthogonal and degenerate, (ii) pseudo-orthogonal and non-degenerate, and (iii) non-orthogonal and non-degenerate respectively, see Fig. 9. The minimum symmetry requirement for a low rotation barrier (via a concerted mechanism) is that the diene provide two pairs of orbitals which approximate orthogonality, but which need not be degenerate. The minimum requirements are provided by the NCP–M interaction. The most important feature contributing to orthogonality loss in the conjugated dienes is the orbital overlap between the 'inner carbons'. The fragment molecular orbitals on the ligand which contribute to the Acceptor 1 and Donor 1 and Donor 2 are shown in Figs. 10–12. Consideration of the symmetry of the ligand FMO45 suggests that Donor 2 will not be affected by deletion of the orbital overlap between the inner carbons as the ligand FMO45 has an orbital node between these carbons. In the case of the Donor 1 interaction the $Fe(CO)_3$ FMO13 is of a_1 symmetry and the interaction with FMO46 should not vary greatly as the ligand and metal rotate relative to one another. Consideration of the Acceptor 1 interaction shows that the ligand FMO44

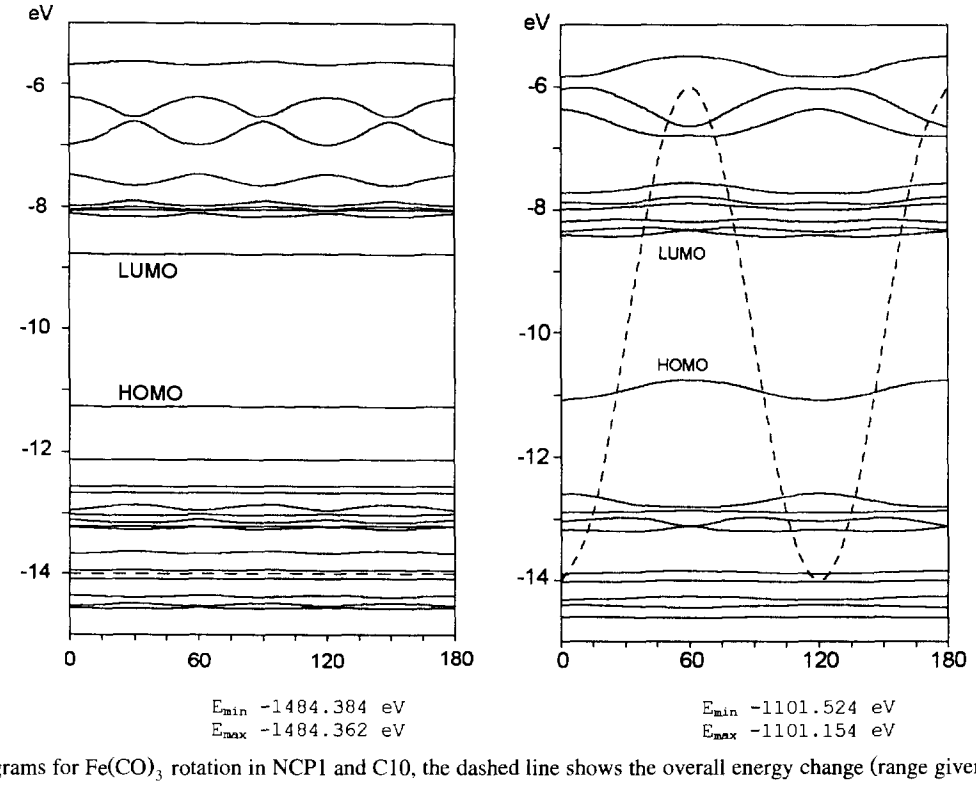

Fig. 8. Walsh diagrams for $Fe(CO)_3$ rotation in NCP1 and C10, the dashed line shows the overall energy change (range given in electron volts).

Table 4
Overlap populations (%) between FMOs and rotation barrier

M = orthogonal $Fe(CO)_3$		Orbital (FMO, s)			Barrier (kcal mol^{-1})	
Compound		Acceptor 1	Donor 1	Donor 2	Calc.	Exp.
(η^4-butadiene)M	C10	30 (14 + 44)	10 (13 + 46)	35 (15 + 45)	8.5	9.1 [54]
(η^4-cycloheptatriene)M	C13	31	8	29	9.0	9.0 [54]
(η^4-1,5-cyclooctadiene)M	NCP1	31	16	30	0.5	[a]
(η^4-norbornadiene)M	NCP4	35	11	32	0.2	[a]

[a] Not measured [1].

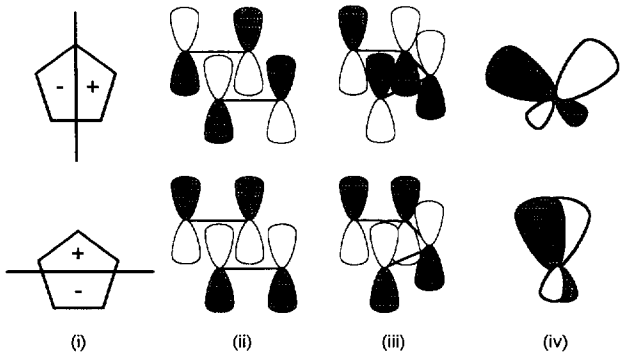

Fig. 9. Generic ligand and metal orbitals.

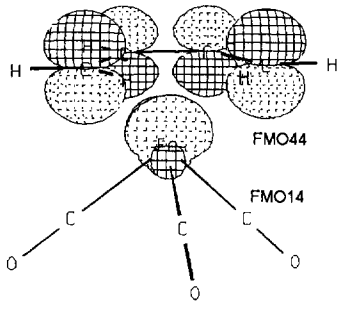

Fig. 10. FMOs for the Acceptor 1 interaction in butadiene $Fe(CO)_3$.

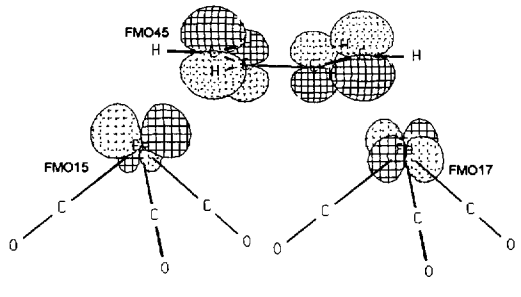

Fig. 11. FMOs for the Donor 2 interaction in butadiene $Fe(CO)_3$.

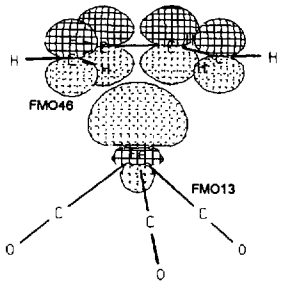

Fig. 12. FMOs for the Donor 1 interaction in butadiene $Fe(CO)_3$.

involved has overlap in the ligand between the inner carbons and has a node between each inner carbon and its neighbouring terminal carbon. This orbital (FMO44) interacts with a metal FMO14 of e symmetry. The MO formed by FMO44 and FMO14 is the metal complex HOMO and follows the energy profile of the Walsh diagram (indicated by the dotted line in Fig. 8) very closely. This suggests that the barrier to rotation is substantially due to the variation in the interaction of this FMO with the metal e orbitals (FMO14) as the ligand rotates. If the overlap between the inner carbons of the ligand is deleted the calculated barrier is reduced to 0.6 kcal mol^{-1}. In contrast, deletion of overlap between a terminal and an inner carbon of C10 has almost no effect on the calculated barrier. Deletion of the overlap between the inner carbons equates chemically to the removal of conjugation in the ligand.

The nature of the interaction between the FMOs of $Fe(CO)_3$ and the butadiene ligand has been explored by Hoffmann and coworkers [21] at the 180° barrier (but not at the 60° or 240° positions), and our work is consistent with that of Hoffmann.

5. Experimental

The unique ligand was often clear and could be determined by rotating the structure on a computer screen until the centroids of the double bonds and two of the monodentate ligands were essentially coplanar. The third monodentate ligand was then the unique one. In more difficult cases the following method was used. 1 and 5 were joined and the resulting line passed through a sector of a disc or ellipsoid defined by either 4–M–* or 4–M–2. The unique ligand is opposite this sector. Having assigned the unique ligand, the larger of the two *trans* angles is defined as $\theta_{1,5}$ and the smaller one as $\theta_{2,4}$.

The other parameter required is $\delta_{2,4}$, the angle between the normals to the faces defined by the ligands 1,2,4 and 5,2,4. Since most software applications which allow the analysis of structures do not specifically measure angles between the faces of a polyhedron, an indirect method was developed to determine $\delta_{2,4}$. Positions 2 and 4 were used to define the centroid D_1, Fig. 13.

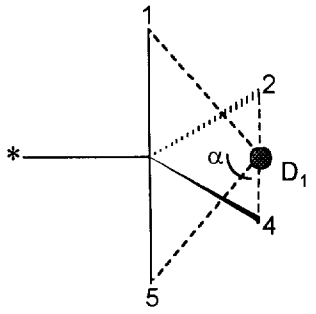

Fig. 13. Construction used to calculate interplanar angles.

D_1 was joined to the axial positions 1 and 5. The lines D_1–1 and D_1–5 lie in the faces 1,2,4 and 5,2,4 respectively. The angle between the normals to the faces $\delta_{2,4}$ is related to the angle α, $\delta_{2,4} = 180 - \alpha$. A final complication in the measurement of $\delta_{2,4}$ arises from the considerable difference between Fe–C and Fe–P bond lengths, approximately 0.4 Å. An ideal square based pyramid will have a $\delta_{2,4}$ value of 0° only if the bond lengths from the metal to the ligands 1,2,4 and 5 are all equal. To circumvent this problem the bonds from the central metal to ligands 1,2,4 and 5 were all set to 2.0 Å. To ensure that this alteration did not affect the value of the angles $\theta_{2,4}$ and $\theta_{1,5}$, the measurement of these angles was made prior to and after the bond length adjustment.

The geometry used for extended Hückel calculations was as follows, the ML_3 fragment was given C_{3V} symmetry with the CO–M–CO angles all at 90°. The distance from the metal to the diene bonding plane was that found in the crystal structure and other bond distances and angles were averaged. The metal atom does not necessarily lie above the centroid of the four η^4 bonding carbons in the ligand. In these calculations the metal atom was offset to lie closer to the terminal carbons of the diene, in accord with the crystallographic data for such compounds. The CACAO package of programs, developed by Mealli and Proserpio [22], was used to perform the extended Hückel calculations. The atomic parameters used are the default values employed in CACAO 4.0. It was necessary to introduce structurally insignificant modifications to the geometry of systems to ensure that the formal symmetry did not change in the generation of Walsh diagrams. A difference in bond angle of 0.1° or bond distance of 0.01 Å is sufficient to remove any increase in symmetry which may occur.

References

[1] F.W. Grevels, J. Jacke, W.E. Klotzbücher, C. Krüger, K. Seevogel and Y. Tsay, *Angew. Chem., Int. Ed. Engl., 26* (1987) 885.
[2] F.W. Grevels, H. Angermund, R. Moser, R. Benn, C. Kruger and J. Rouaou, *Organometallics, 7* (1988) 1994.
[3] K.S. Claire, O.W. Howarth and A. McCamley, *J. Chem. Soc., Dalton Trans.*, (1994) 2615.
[4] J.J. Turner, F.W. Grevels, S.M. Howdle, J. Jacke, M.T. Haward and W.E. Klotzbücher, *J. Am. Chem. Soc., 113* (1991) 8347.
[5] P. McArdle, D. Cunningham, T. Higgins, W. Corrigan, R. Foley and A.R. Manning, *J. Organomet. Chem., 479* (1994) 63.
[6] O.S. Mills and G. Robinson, *Acta Crystallogr., 16* (1963) 758.
[7] T.A. Albright, P. Hoffmann and R. Hoffmann, *J. Am. Chem. Soc., 99* (1977) 7546.
[8] L. Kruczynski and J. Takats, *J. Am. Chem. Soc., 96* (1974) 932.
[9] J.A.S. Howell, G. Walton, M.C. Tirvengadum, A.D. Squib, M.G. Palin, P. McArdle, D. Cunningham, Z. Goldschmidt, H. Gottlieb and G. Strul, *J. Organomet. Chem., 401* (1991) 91.
[10] D. Cunningham, T. Higgins, P. McArdle, W. Corrigan and A.R. Manning, *J. Organomet. Chem., 479* (1994) 103.
[11] J.A.S. Howell, A.G. Bell, P.J. O'Leary, G.R. Stephenson, M. Hastings, P.W. Howard, D.A. Owen, A.J. Whitehead, P. McArdle and D. Cunningham, *Organometallics, 15* (1996) 4247.
[12] R.R. Holmes, *Acc. Chem. Res., 12* (1979) 257.
[13] A.R. Rossi and R. Hoffmann, *Inorg. Chem., 14* (1975) 365.
[14] R.R. Holmes, R.O. Day, J.J. Harland, A.C. Sau and J.M. Holmes, *Organometallics, 3* (1984) 341.
[15] T.P.E. AufderHeyde, *Angew. Chem., Int. Ed. Engl., 33* (1994) 823.
[16] J.Z. Zeemann, *Z. Anorg. Allg. Chem., 324* (1963) 241.
[17] D.L. Kepert, *Inorg. Chem., 12* (1973) 1938, 1942.
[18] F.M. Chaudhari and P.L. Pauson, *J. Organomet. Chem., 5* (1966) 73.
[19] T.A. Albright, R. Hoffmann and P. Hoffmann, *Chem. Ber., 111* (1978) 1591.
[20] R.J. Buenker and S.D. Peyerimhoff, *Chem. Rev., 74* (1974) 127.
[21] T.A. Albright, R. Hoffmann and P. Hoffmann, *Chem. Ber., 111* (1978) 1591.
[22] C. Mealli and D.M. Proserpio, *J. Chem. Ed., 67* (1990) 399.
[23] N. Sakai, K. Mashima, H. Takaya, R. Yamaguchi and S. Kozima, *J. Organomet. Chem., 181* (1991) 419.
[24] G.R. Stephenson, M. Hastings, P.W. Howard, D.A. Owen, A.J. Whitehead, J.A.S. Howell, A.G. Bell, P.J. O'Leary, P. McArdle and D. Cunningham, *Organometallics*, in press.
[25] A. Bond, *J. Chem. Soc., Dalton Trans.*, (1977) 2372.
[26] F.A. Cotton and J.M. Troup, *J. Organomet. Chem., 212* (1981) 411.
[27] P. Vogel, *J. Organomet. Chem., 89* (1979) 174.
[28] A. Hafner, *Helv. Chim. Acta, 72* (1989) 168.
[29] P. Vogel, *Helv. Chim. Acta, 64* (1981) 2328.
[30] S.M. Johnson and I.C. Paul, *J. Chem. Soc. (B)*, (1970) 1784.
[31] J.A.S. Howell, A.G. Bell, P.J. O'Leary, P. McArdle, D. Cunningham, G.R. Stephenson and M. Hastings, *Organometallics, 13* (1994) 1806.
[32] Z. Goldschmidt, *J. Organomet. Chem., 301* (1986) 337.
[33] J. Howell, M.C. Tirvengadum, A.D. Squib, G. Walton, P. McArdle and D. Cunningham, *J. Organomet. Chem., 347* (1988) C5.
[34] J.A.D. Jeffreys and C. Metters, *J. Chem. Soc., Dalton Trans.*, (1977) 729.
[35] K. Broadley, N.G. Connelly, R.M. Mills, M.W. Whiteley and P. Woodward, *J. Chem. Soc., Chem. Commun.*, (1981) 19.
[36] A. Gieren and W. Hoppe, *Acta Crystallogr., B28* (1972) 2766.
[37] J. Skelton, *Thesis*, University College, Galway, 1995.
[38] A.J. Pearson and P.R. Raithby, *J. Chem. Soc., Dalton Trans.*, (1981) 884.
[39] G.E. Herberich, *Chem. Ber., 110* (1977) 760.
[40] D.I. Woodhouse, G.A. Sim and J.G. Sime, *J. Chem. Soc., Dalton Trans.*, (1974) 1331.
[41] V.G. Andrianov, *Izv. Akad. Nauk SSSR, Ser. Khim.*, (1985) 590.
[42] R. Goddard and P. Woodward, *J. Chem. Soc., Dalton Trans.*, (1979) 711.

[43] A.S. Batsanov, *Koord. Khim., 13* (1987) 1551.
[44] M.G. Waite and G.A. Sim, *J. Chem. Soc. (A)*, (1971) 1009.
[45] A. Dunand and G.B. Robertson, *Acta Crystallogr., B38* (1982) 2038.
[46] J. Fischer and L. Ricard, *Acta Crystallogr., B38* (1982) 1140.
[47] R.B. King, *J. Chem. Soc., Chem. Commun.*, (1979) 10.
[48] L.A. Paquette, *Organometallics, 8* (1989) 2167.
[49] A.J. Pearson, *Organometallics, 11* (1992) 4096.
[50] H. Irngartinger, T. Oeser and C.M. Kohler, *Acta Crystallogr., C49* (1993) 378.
[51] A.V. Rivera and G.M. Sheldrick, *Acta Crystallogr., B34* (1978) 3374.
[52] W.H. Whatson, *Acta Crystallogr., C46* (1990) 24.
[53] F.W. Grevels, *Z. Naturforsch., 35b* (1980) 360.
[54] L. Kruczynski and J. Takats, *Inorg. Chem., 15* (1976) 3140.